Elastic Energy Storage in Planar Robot Throwing Arm

Alexander Rowe(*Author*)
Joshua Sullivan (*Author*)
Simon Walker (*Author*)
Dr Martin Stoelen (*Co-Author*)
Dr Jonathon Marsden (*Co-Author*)
School of Computing and Mathematics
Plymouth University
Plymouth, UK

***Abstract*— Humans are particularly good at throwing, in part due to their ability to store and then suddenly release energy in tendons. It is suggested that by adding artificial elastic tendons to a planar robotic arm, it will be able to throw further than if each joint was statically connected. Further by studying and imitating the motion of a human throw, it is hoped the maximum amount of energy storage and release can be obtained.**

Keywords—elastic; energy; storage; tendon; power;

I. INTRODUCTION

The aim of this project was to design and build a ball throwing robot. This robot is able to launch a projectile using energy from actuators built into the arm as well as utilising a form of elastic energy storage.

Two core design methodologies were used for the arm, the first being designing an arm that is optimal for throwing from an engineering standpoint. The second aiming to replicate the design and motion of a human arm.

The arm consists of a shoulder, elbow and wrist joint. To best emulate a human, the movement of the joints is constrained to that of a human arm. To further reduce complexity, the arm is restricted to movement in one plane. The movement of the arm is controlled via tendons connected separately to two servos at each joint, this enables it to store energy and release it suddenly. Figure 1 shows the arm with all the servos and spools in place.

By having the servos connected via soft tendons, instead of statically to each joint, more energy is stored and the robotic arm can move at a higher speed than a solid robot arm. This is supported by conclusions drawn from D. J. Braun et al.

"Variable stiffness throwing provides a clear performance benefit compared to the corresponding fixed stiffness case" [1]

This project encompasses skills from a variety of areas. These include Computer Aided Design (CAD), Computer Aided Manufacturing (CAM), tensile/hardness testing, agonist-antagonist joints, and soft mechanisms and materials.

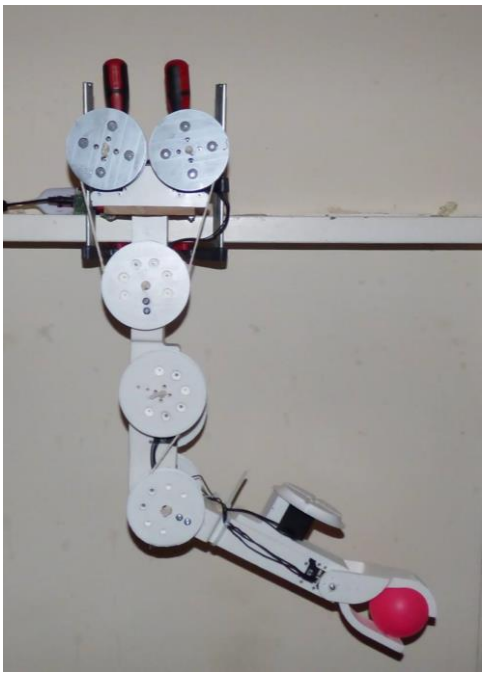

Figure 1 – Robot Arm

II. CURRENT WORK

The university of Pisa are currently working with QBrobotics variable stiffness servos to create a ball throwing robot arm. The softness of each of these servos however is solely dependent on the compliance in the servos with their mechanical variable stiffness ranging from 0.5 -13 Nm rad^{-1}. [2] Their research has demonstrated that more energy can be exploited by using servos with mechanical compliance. [3]

III. DESIGN PROCESS

A. Human Body

1) Joint location and Spacing

The soft robotic arm has been created to imitate a human throw using artificial tendons. The dimensions of the arm were taken from a NASA report, recording the dimensions of an average sized Japanese lady. The arm consists of two joints, the shoulder and the elbow, with the wrist being a rigid extension of the lower arm. The upper arm has a length of 272-324mm and the lower arm 373-446mm. [4]

2) Co-Contraction

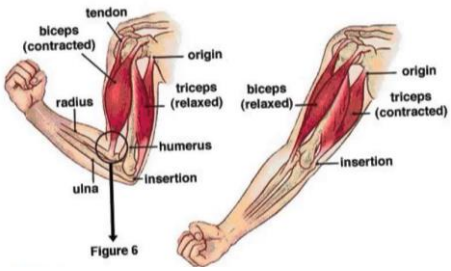

Figure 2 - Anatomical Representation of Human Arm [5]

As shown in Figure 2, the human arm uses antagonistic muscle pairs working in opposition to each other to control the movement; as one muscle contracts, the other relaxes. This type of energy storage means the human arm is excellent at throwing projectiles and is why it was chosen to be replicated in this project.

B. CAD

Autodesk Fusion 360 was used as the CAD software for this project because it is designed for collaborative working, is easy to use, and free for academic use.

Each part of the arm has been designed so it will fit onto most standard 3D printers. Further to this, some parts such as the spools and pivots have been designed from the same starting part. This re-use of design sped up the development process.

A full list of parts includes

1. Shoulder joint
2. Arm upper section
3. Arm lover section
4. Lower Gripper
5. Upper Gripper
6. MX64 Spools
7. AX64 Spools
8. MX64 Spacers
9. AX64 Spacers
10. Elbow Pivot
11. Shoulder Pivot

A .iges CAD file can be found in the project's GitHub repository containing all of these parts [6].

C. Arm Geometry

Figure 3 shows a full geometric drawing of the arm, on the left from the front and on the right from the side. The tendons, in orange, link the servo spools to the next arm section. Two servos have been used as encoders in the elbow and shoulder joint. A ball is situated in the gripper.

The length of the upper arm is taken from the join in the shoulder to the joint in the elbow, the length of the lower arm is taken from the joint in the elbow to the end of the gripper.

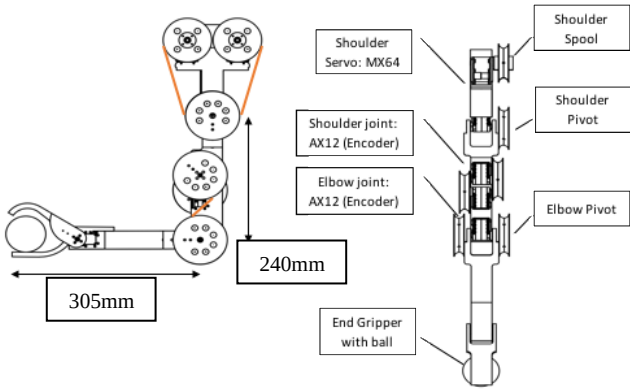

Figure 3 - Geometric drawing of the robot arm. (Front and Side)

IV. IMPLEMENTATION

A. Computer Aided Manufacture (CAM)

1) Laser Cutting

A laser cutter was used to create a medium density fiberboard (MDF) mounting plate that the shoulder piece slots into. Laser cutting was used because it is extremely fast and precise.

2) 3D Printing

With the exception of the servos and bolts, all other parts were 3D printed. This allowed for a rapid development cycle of printing, testing, modifying the design, and reprinting. This evolutionary design process allows errors to be spotted much earlier than they otherwise would.

B. Soft Mechanisms & Materials

The arm can be considered a "soft robot" as it uses flexible tendons made from Semiflex filament wrapped in nylon for energy storage. The testing and selection of the tendon material are discussed in section VI.A Tendon Testing.

Semiflex is a flexible material that can elongate to 600% of its original length before breaking and 49% to yield. Semiflex is cylindrical with a diameter of 3mm. [7]

Nylon is a firm material that can elongate to 150% of its original length before breaking, and 105% to yield. [8] The nylon thread is cylindrical with a diameter of 0.5mm

C. Hardware

All chassis components are constructed of 3D printed PLA plastic. The "shoulder" and "elbow" joints of the arm are Dynamixel AX-12 servos, with their drive gears removed. This enables them to be used as rotational encoders.

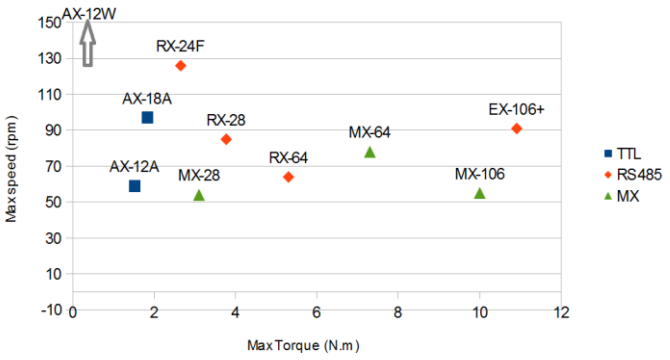

Figure 4 - Torque and Speed Comparison of Dynamixel Servos [9]

The upper drive servos are Dynamixel MX-64T servos, chosen for their high torque as shown in Figure 4. All other servos are Dynamixel AX-12As, chosen for their light weight and cost effectiveness.

D. Control

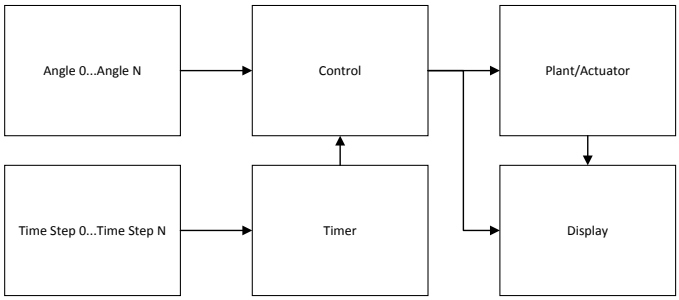

Figure 5 - Control Diagram

The motion of the arm is controlled using a variation on the "Bang-Bang" (hysteresis) controller. The arm has a sequence of seven set positions, which it attempts to reach one after the other, with the joint angles and time delay between each step variable. This is shown in Figure 5. This controller was written in National Instruments LabVIEW, using the Dynamixel API [10]

Each servo has its own PID controller within it; the controlling computer simply sends the desired position to it, and the servo moves to that position.

This control strategy was chosen for its simplicity and speed of development; however, it has several drawbacks. Although the timings were based on timings of a human throw, it quickly became clear that this throw was sub-optimal. Because this becomes an optimisation problem, it makes this control strategy suitable for a machine learning solution.

V. Analysis

An analysis was made on the arm to calculate what torque was required from the servos to hold the arm horizontally. All weight has been taken into account including a ball weighing 157g attached to the end.

A. Assumptions

I. The weight of the arm has been split into the weight of the PLA and the weight of the servos. This is because the servos contribute a lot to the overall weight and also because they are not uniformly distributed over the arm. The weight of the plastic will be considered as being uniformly distributed.

II. The servo spool and the Shoulder pivot are assumed to be directly above one another.

III. The Servos and ball are placed in the center of the arm instead of on top of the arm.

B. Free Body Diagrams

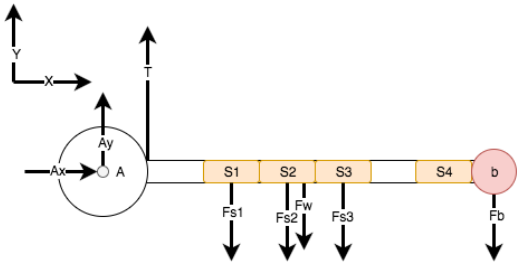

Figure 6 – Free Body Diagram 1, Full Arm

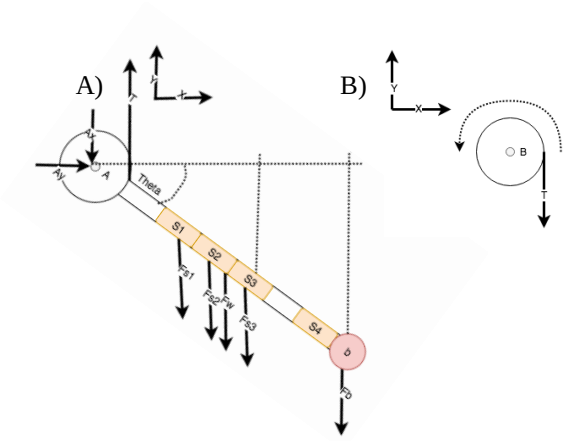

Figure 7 – A) Free Body Diagram 2, Full arm at 28 degrees B) Free Body Diagram 3, shoulder servo

C. Equations

$$\sum M_A = (T * R) - (F_{s1} * D_1) - (F_{s2} * D_2) - \left(F_w * \frac{D_0}{2}\right) - (F_{s3} * D_3) - (F_{s4} * D_4) - (F_B * D_0)$$

$$T = \frac{0.06 + 0.077 + 1.465 + 0.13 + 0.243 + 0.8855}{35 * 10^{-3}}$$

$$T = 67.29N$$

$$\sum M_B = T * 35 * 10^{-3}$$

$$M_B = 2.0792Nm$$

$$T = \frac{0.0529 + 0.6824 + 1.356 + 0.114 + 0.2142 + 0.78078}{30.9 * 10^{-3}}$$

$$T = 60.47N$$

$$\sum M_B = T * 30.9 * 10^{-3}$$

$$M_B = 1.868Nm$$

The positive force direction upwards, the positive moment direction is counter-clockwise. The first equation is used to calculate the sum of the moment around A. This is done for both the arm holding the ball horizontally and also at 28 degrees from horizontal.

Tension (T) is then found by rearranging the formula. Once T has been identified the moment around B in Figure 7 (B). can be calculated.

D. Discussion

The torque required from the servo to support the arm horizontally was calculated to be 2.0792Nm. The torque required to support the arm at 28 degrees below the horizontal was calculated to be 1.868Nm.

The stall torque of the MX64 servo is 6.0Nm. Robotis recommends that for a controlled motion, only 1/5th of the stall torque should be used [11]. The arm was unable to support the arm horizontally however it was able to support the arm at 28 degrees below the horizontal. This shows the relative strength of the servos against the weight of the ball and could be comparable to a human holding a bowling ball.

VI. Experiments

A. Tendon Testing

1) Method

An Instron tensile testing machine was used to analyse the properties of various tendon types whilst under tension. Each tendon had identical lengths so only the difference in elasticity/plasticity is measured. Seven different tendons were tested, Semiflex and Silicon wrapped with Nylon (Medium, Tight), standard Semiflex and Silicon and PLA. Semiflex and Silicon were chosen due to their elastic nature, the additional of nylon is to stop the materials from plasticity.

2) Results

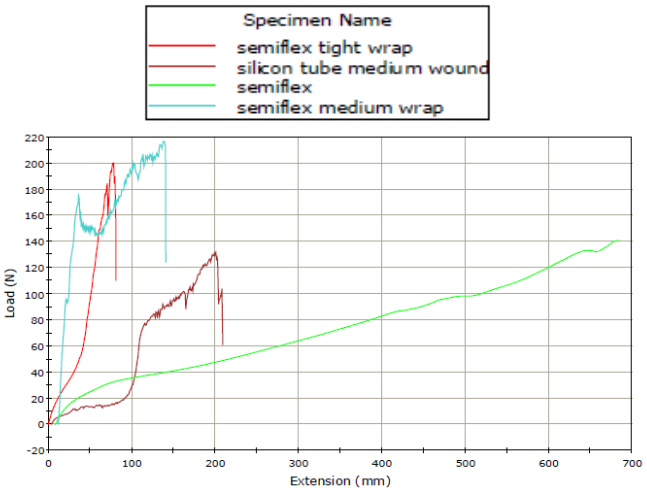

Figure 8 - Tendon Specimens 1- 4 (Loads vs Extension)

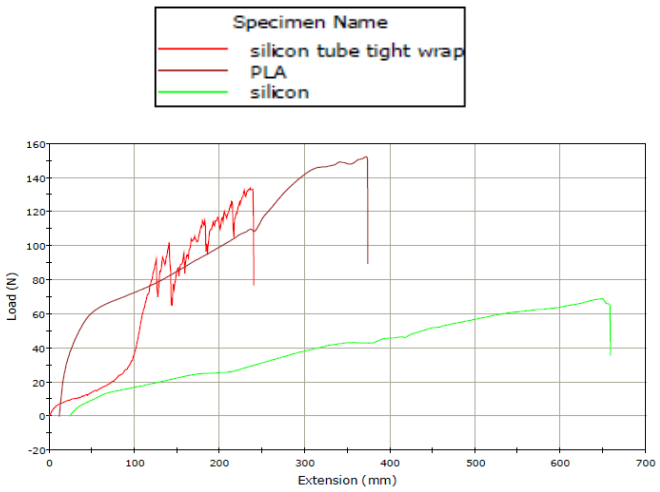

Figure 9 - Tendon Specimens 5-7 (Load vs Extension)

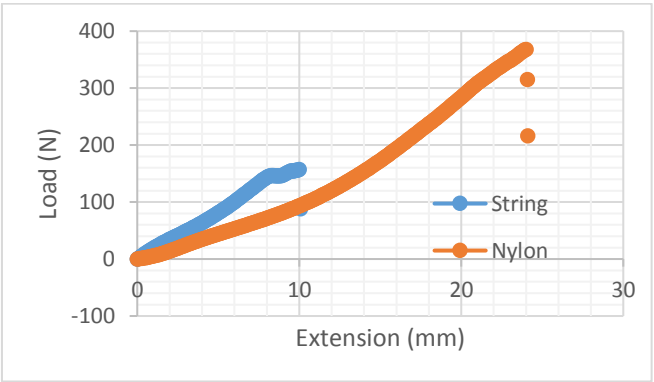

Figure 10 - Nylon Thread and String Load vs Extension Graph

The force vs extension profiles of several potential tendon materials are shown in Figure 8, Figure 9 and Figure 10. Semiflex and Silicon both have large extensions vs their loads. The addition of nylon wrapped around both materials meant they could hold higher loads and reduced the amount of extension. The jagged edges can be attributed so a small amount of slippage from the tendons. All of the tendons were tested until they fractured, suffered from plasticity or the machine could not extend any further.

Figure 10 shows the force vs extension profiles for Nylon and string. Both the Nylon and the String can take a large load with little extension.

3) Discussion

From this data, a tendon made of Semiflex filament, wrapped tightly with nylon fishing wire was selected. This tendon was chosen due to its exponential characteristics displayed on the graph. It also has a large elastic region and was able to hold a load of 200Ns before breaking or reaching its' elastic limit. Silicon and Semiflex alone would have been too elastic, giving too much extension vs the load.

Nylon was chosen to wrap around the Semiflex due to its ability to hold high loads with little extension. The String will be used instead of the Semiflex when comparing a hard throw against a soft throw.

B. Comparing a Human Arm to Robot Arm Throw

1) Method

To better understand how a human throws a projectile a study was undertaken at the Plymouth Human Movement and Function Laboratory (HMFL). Using two Infrared transmitters on each joint and two cameras a 2D simulation was created of the arm throwing. This enabled a detailed analysis of the movements, angles, accelerations and velocities experienced during the throw to be created. This data enabled a throw to be created that accurately recreated a human throw.

A video camera was set up above, in front and to the side of the arm to allow for a visual comparison in addition to the data collected from the sensors.

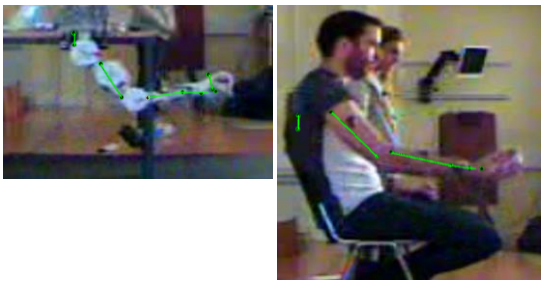

Figure 11 - Robot and Human Arms Compared at Human Movement and Function Laboratory

Each joint is fitted with two sensors. The first two sensors are for the Proximal Scapular to the distal Scapular. The second set of sensors is for the Proximal humorous to the Distal Humorous and the third set of sensors is for the Proximal Radius to Distal Radius. Two sensors where attached to the ball to record its motion as it left the hand. The sensors are located at either end of each green line in Figure 11.

2) Results

Figure 12, Figure 13 and Figure 14 show the human motion of throwing an arm. Figure 12 displays the tracking of the sensors mounted on the arm and the trajectory travelled by the ball

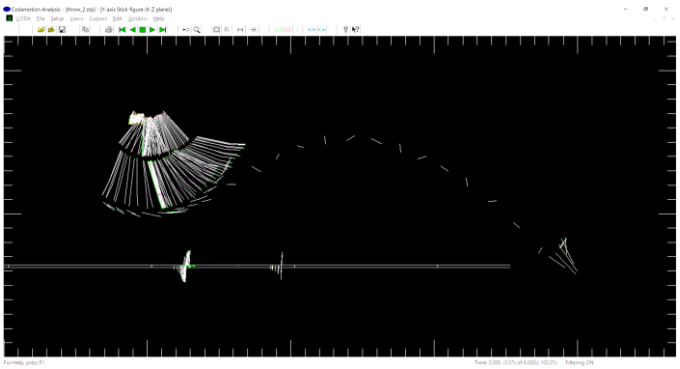

Figure 12 - Model of Human Throw

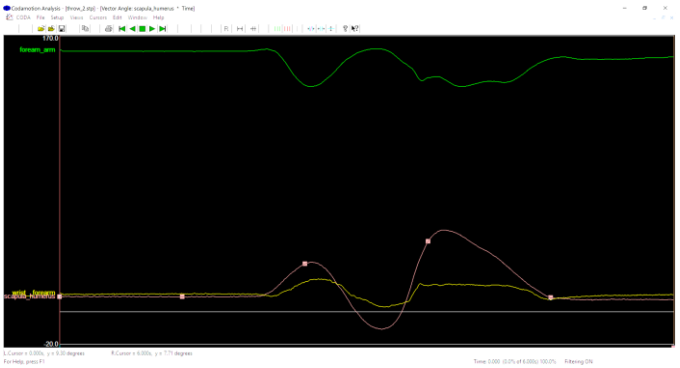

Figure 13 - Human Arm Vector Angles

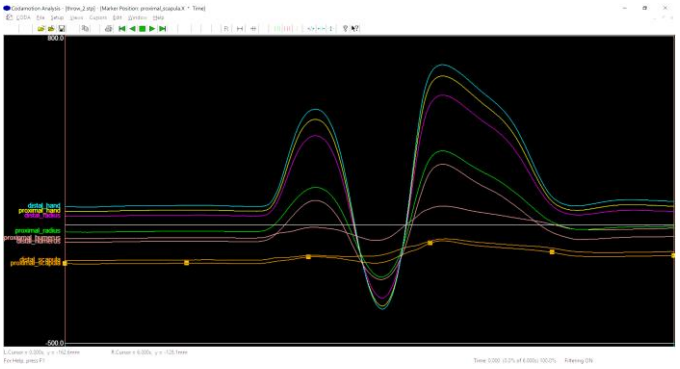

Figure 14 - Human Arm Joint Positions

Figure 15, Figure 16 and Figure 17 show the human motion of throwing an arm. Figure 15 displays the tracking of the sensors mounted on the arm and the trajectory travelled by the ball.

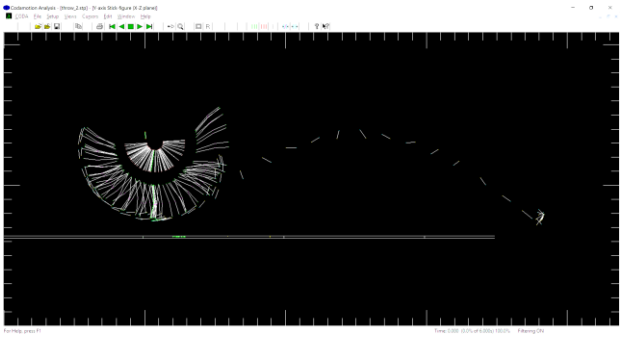

Figure 15 - Model of Robot Throw

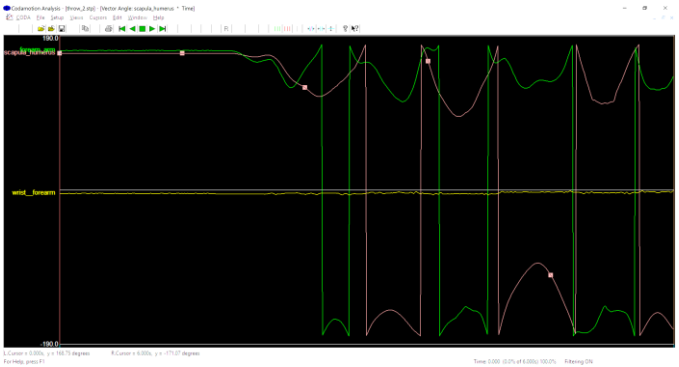

Figure 16 - Robot Arm Vector Angles

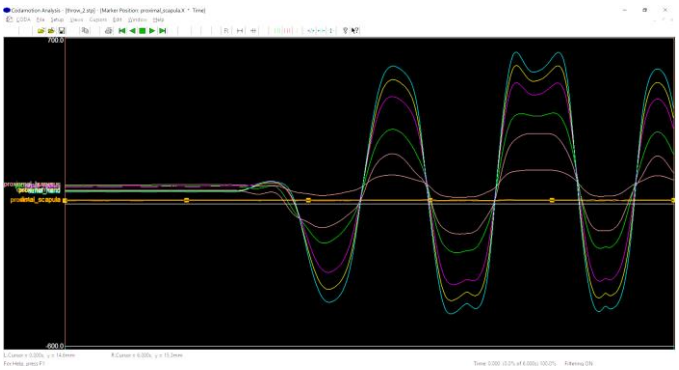

Figure 17 - Robot Arm Joint Positions

3) Discussion

The human throw is a perfect example of energy storage being transferred through antagonistic muscle pairs to propel a projectile through the air. It was logical to try and replicate a human throw with the robot arm. Both throws ended up being quite similar however once the arm was built it was clear where improvements could be made to produce a better throw.

To replicate the throw of a human arm, the angles were taken from Figure 13, and used to design the robot gait. This is why the throws shown in Figure 12 and Figure 15 are very similar. The only difference being that the robot throw has an additional swing in it, leading to the extra oscillation in the angle and joint position charts (Figure 13 and Figure 16).

C. Compliant tendons vs non-compliant tendons

1) Method

The effectiveness of the throw is measured via the distance it can throw the projectile. Two throws were measured and compared against each other, a ‘soft’ throw and a ‘hard’ throw. The soft throw was achieved using the elastic tendons, these were then swapped for ones with no compliance so a comparable hard throw could be achieved. The ball was then thrown 50 times for each and the distances measured. The horizontal distance has not been measured.

The arms throw has been optimised to get the best throw from using the elastic tendons. The arm attempts to build up energy in the tendons by tightening the spools before the full extent of the swing has completed. If the arm tried to replicate this method with static tendons it could damage the servos or the arm so this was removed in the hard throw. An attempt to keep the throw as similar to each other as possible was made so they could be compared.

The arm was attached to a table with paper laid out on the floor in front of it. The ball was covered with ink so as it hit the ground the mark left would show where the ball landed. This gave a reliable method to accurately and precisely record the distance.

2) Results

Figure 18 shows a histogram of the recorded throws. The X axis is the bins ranging from 2040 to 2711 in jumps of 61mm. The Y axis is the frequency to which a ball landed within that range. Both throws display a normal distribution with the hard throws centre of distribution at 2284 and the soft throw at 2589. The spread was calculated at 610 and 330 respectively.

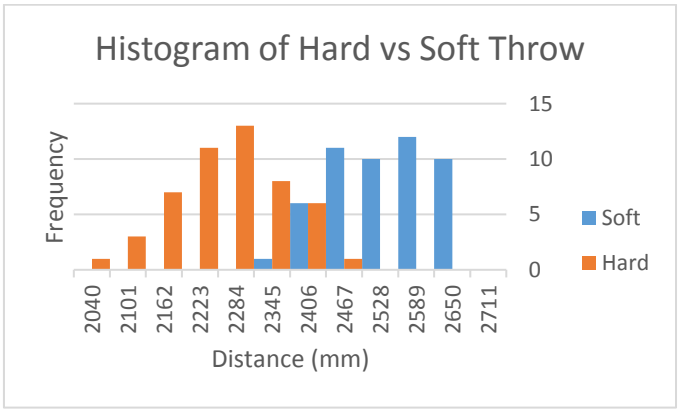

Figure 18 - Histogram of Hard vs Soft Throw

The average distance achieved by the hard throw 2508.9mm was and the soft throw was 2231.9mm.

	Soft Distance (mm)	Hard Distance (mm)	All Data (mm)
Mean	2508.9	2231.9	2370.4
Median	2497.5	2240	2387.5
Range	330	375	600
Mode	2470	2240	2470

Table 1 - Mean, Median, Range and Mode for Soft, Hard and Combined Throws

Table 1 shows the mean, median, range and mode for both the hard and the soft throw. The "All Data" column shows a combination of both throws. The soft throw has a higher average, median and mode. The hard throw has a larger range of 375.

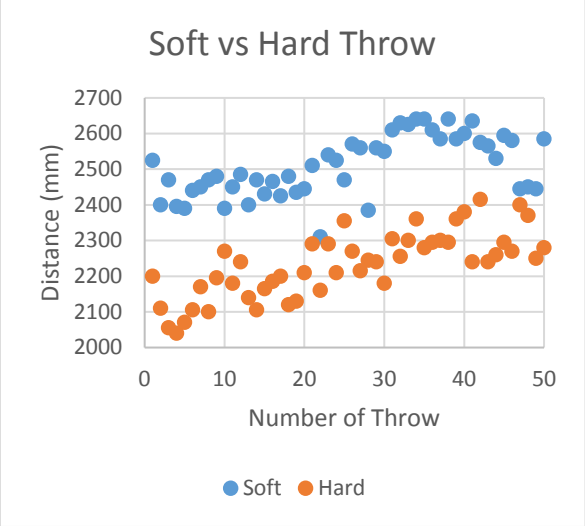

Figure 19 – Soft Vs Hard throw distance

Figure 19 shows the distance reached by each throw. In blue is the soft throws and in orange the hard throws. Unusually it was noted that both throws had an upwards trend as they progressed through their throws.

3) Discussion

The test data shows how the soft throw achieved a further throw than the hard throw. Additional energy was added to the system via the tension in the soft tendons as the arm tightened the spools. This enabled it to on average throw further than when it was statically connected.

The robot managed to throw 100 times with a range between 330 and 375. This range shows how the arm can perform precise throws again and again.

It was noted that the even though the elastic storage added additional energy to the system the majority of the power was coming from the MX-64 Servos. This is why the distance difference is relatively small.

D. Enegry storage in the arm

1) Method

A second test of the tendons in the arm shows the amount of extension as the arm throws. This shows if energy is being stored and released during the throw.

Two tabs were attached to the tendon that connects the right shoulder spool (Front View) to the shoulder pivot. A video camera was set up with a rule behind to measure the extension as the throw commenced.

2) Results

Figure 20 demonstrates the extension of the tendon during a throw. The image on the left of the figure is before the throw has started, the length between the two markers is 110mm. The image on the right is during the build up phase of the main swing. The shoulder servo is winding in the tendon while the arm is still swinging backwards to store energy. This is when the tendon is at its maximum extension of 141mm. This gives a difference of 41mm over the test area and shows that the robot is making use of energy storage.

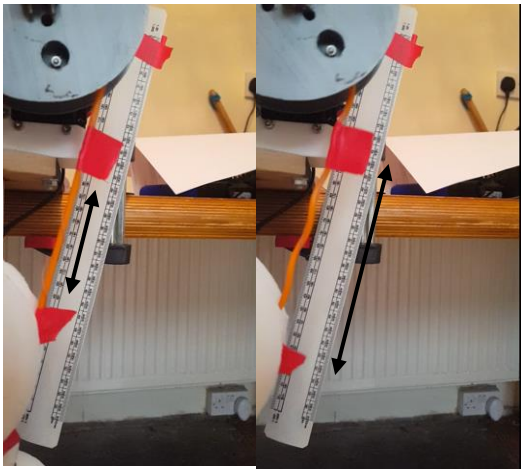

Figure 20- Tendon Extension during throw

3) Discussion

The difference in extensions recorded, on the tendons, shows that arm is using the tendons to store energy. The image on the right of Figure 11 also shows how that as the tension builds on the tendons the nylon wrapped around the Semiflex tightens causing the Semiflex to bend. This is why the tendon appears to be wavy.

VII. Conclusion

This robot successfully made use of elastic energy storage, achieving this through its artificial tendons. The exponential nature of the tendons enabled the robot to throw a ball further than when the joints had been statically linked. It was clear to see during the throw that the extension of the tendons was changing with the load, building up energy as the arm swung back, and releasing it explosively as it came forward.

Using rapid prototyping, the timescale for the development of the hardware required for this project was greatly reduced.

The movement of the arm was modelled on that of a human, giving a good starting point for gait design, however, it was sub-optimal. The gait was somewhat improved by increasing the shoulder tendon tension and increasing elbow speed, however, because the throw is an optimisation problem, it makes it a good candidate for machine learning.

Further improvements to this project could include adding an adjustment value for co-contraction of the tendons, and adding strain sensors to each tendon. This would give more control over the system and greater feedback.

VIII. References

[1] D. J. Braun, M. Howard and S. Vijayakumar, "Exploiting Variable Stiffness in Explosive Movement Tasks," *Robotics: Science and Systems VII*, p. 25, 2012.

[2] QBRobotoics , "QBMOVE MAKER PRO," [Online]. Available: http://www.qbrobotics.com/products/qbmove-maker-pro/. [Accessed 16 10 2016].

[3] Centro di Ricerca Enrico Piaggio, "Hammering with a qbmove maker pro," Pisa , 2015.

[4] NASA, "NASA-STD-3000,," July 1995. [Online]. Available: https://msis.jsc.nasa.gov/default.htm. [Accessed 17 December 2016].

[5] J. Stoppani, "Antagonist Muscle Pairs," 29 11 2012. [Online]. Available: http://xbodyconcepts.com/antagonist-muscle-pairs/. [Accessed 11 12 2016].

[6] A. Rowe, J. Sullivan and S. Walker, "2016-group4/Complete Arm v27.iges," 11 01 2017. [Online]. Available: https://github.com/ROCO504/2016-group4. [Accessed 11 1 2017].

[7] NinjaTek, "Techincal Specfication," 04 2016. [Online]. Available: https://ninjatek.com/wp-content/uploads/2016/05/SemiFlex-TDS.pdf.

[8] theplasticshop.co.uk, "nylon 66 technical data sheet," 2011. [Online]. Available: https://www.theplasticshop.co.uk/plastic_technical_data_sheets/nylon_66_technical_data_sheet.pdf. [Accessed 11 01 2017].

[9] Generation Robots, "Dynamixel AX-12A Actuator," [Online]. Available: https://www.generationrobots.com/en/401075-dynamixel-ax-12-a-actuator-robotis.html. [Accessed 2017].

[10] National Instruments, "Index of /evaluation/labview/lvtn/vipm," 06 01 2017. [Online]. Available: http://download.ni.com/evaluation/labview/lvtn/vipm/. [Accessed 11 2016].

[11] Trossen Robotics, "Dynamixel MX-64T Robot Actuator," 2017. [Online]. Available: http://www.trossenrobotics.com/p/mx-64t-dynamixel-robot-actuator.aspx.